JOC*Article*

New Method for the Synthesis of *N*-*tert*-Alkoxyarylaminyl Radicals[1]

Yozo Miura,*,† Yoshikazu Muranaka,† and Yoshio Teki‡

Department of Applied Chemistry, Graduate School of Engineering, Osaka City University, Sumiyoshi-ku, Osaka 558-8585, Japan, and Department of Material Science, Graduate School of Science, Osaka City University, Sumiyoshi-ku, Osaka 558-8585, Japan

miura@a-chem.eng.osaka-cu.ac.jp

Received January 17, 2006

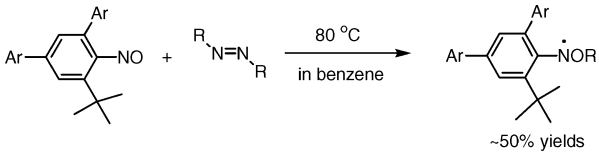

Ar = Ph, R = $C(Me_2)COOCH_3$
Ar = Ph, R = $C(CN)(Me)CH_2CH(Me)CH_3$
Ar = Ph, R = $C(CN)(Me)CH_2C(OMe)(Me)CH_3$
Ar = 4-ClC_6H_4, R = $C(CN)(Me)CH_2CH(Me)CH_3$

The reactions of 2,4-diaryl-6-*tert*-butylnitrosobenzenes with 2,2′-azobis[2-(methoxycarbonyl)propane] (**5a**), 2,2′-azobis(2-cyano-4-methylpentane) (**5b**), and 2,2′-azobis(2-cyano-4-methyl-4-methoxypentane) (**5c**) in refluxing benzene gave stable *N*-*tert*-alkoxy-2,4-diaryl-6-*tert*-butylphenylaminyls, which were successfully isolated as radical crystals in 13−52% yields after column chromatography. The radical yields depended on the reaction time and the molar ratio of azo compounds to nitroso compounds. In the same manner, acetyl- and cyano-group-carrying *N*-*tert*-alkoxyarylaminyls were generated by the reaction of 2-phenyl-4-(4-acetylphenyl)-6-*tert*-butylnitrosobenzene and 2-phenyl-4-(4-cyanophenyl)-6-*tert*-butylnitrosobenzene with **5a** and **5b**, and they were isolated as radical crystals. X-ray crystallographic analyses were performed for two radicals, and their molecular structures were discussed in detail. The magnetic properties were measured for the two isolated radicals with SQUID in the temperature range 1.8−300 K. One radical showed a weak ferromagnetic interaction ($\theta = 0.2$ K) between the radicals, and the other showed a weak antiferromagnetic interaction ($\theta = -3.8$ K). The ferromagnetic interaction was analyzed based on the X-ray crystallographic structure.

Introduction

Although a variety of *N*-alkoxyalkylaminyls (RṄOR′) and *N*-alkoxyarylaminyls (RṄOAr) have widely been investigated by ESR spectroscopy, their isolation has been unsuccessful for a long time.[2] This has been in contrast to the chemistry of thioaminyl (RṄSR′). Thioaminyls are the sulfur analogues of *N*-alkoxyaminyls, and a variety of thioaminyls have been isolated as radical crystals.[3] However, quite recently we found that *N*-alkoxyarylaminyls **1**−**3** can be successfully isolated as radical crystals.[4] This was the first isolation of *N*-alkoxyarylaminyls. Interestingly, the *N*-*tert*-alkoxyarylaminyls are thermally very stable and do not react with oxygen.[1,4−7] In recent years, the isolable, stable, free radicals have attracted much attention as the spin source and building blocks in the study on organic magnetism.[8−10] Radicals **1**−**3** were generated by the

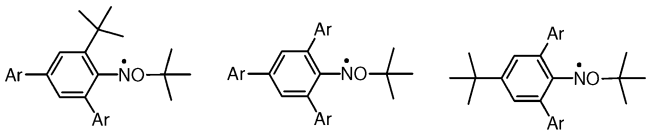

reaction of the lithium salts of the corresponding 2,4,6-

* To whom correspondence should be addressed. Phone: +81-6-6605-2798. Fax: +81-6-6605-2769.
† Graduate School of Engineering.
‡ Graduate School of Science.

(1) ESR Studies of Nitrogen-Centered Free Radicals. 60. For part 59, see: Miura, Y.; Nishi, T. Y. *J. Org. Chem*. **2005**, *70*, 4177.

(2) Danen, W. C.; Neugebauer, F. A. *Angew. Chem., Int. Ed. Engl*. **1975**, *14*, 783. Danen, W. C.; West, C. T.; Kensler, T. T. *J. Am. Chem. Soc*. **1973**, *95*, 5716. Kaba, R. A.; Ingold, K. U. *J. Am. Chem. Soc*. **1976**, *98*, 7375. Woynar, H.; Ingold, K. U. *J. Am. Chem. Soc*. **1980**, *102*, 3813. Ahrens, W.; Wieser, K.; Berndt, A. *Tetrahedron Lett*. **1973**, 3141. Balaban, A. T.; Frangopol, P. T.; Frangopol, M.; Negoiță, N. *Tetrahedron* **1967**, *23*, 4661. Negoita, N.; Baican, R.; Balaban, A. T. *Tetrahedron Lett*. **1973**, 1877. Ahrens, W.; Berndt, A. *Tetrahedron Lett*. **1973**, 4281. Negareche, M.; Boyer, M.; Tordo, P. *Tetrahedron Lett*. **1981**, *22*, 2879.

10.1021/jo0600959 CCC: $33.50
Published on Web 05/23/2006

trisubstituted anilines with *tert*-alkylperoxybenzoates in THF at −78 °C.[1,4−7] Although the above method is convenient, there are some problems. For example, the isolated radical yields are low,[1,4−7] (12−27%) and the use of butyllithium in the radical syntheses refuses the presence of functional groups. To overcome these problems, much effort has been paid, and we have now established a new convenient method for the synthesis of *N*-*tert*-alkoxyarylaminyls.[11] The method involves the addition of a *tert*-alkyl radical to 2,4-diaryl-6-*tert*-butylnitrosobenzenes. Because *tert*-alkyl radicals can be conveniently generated by thermolysis of azo compounds, the procedure for the synthesis of *N*-*tert*-alkoxyarylaminyls is only to heat solutions of nitrosobenzenes and azo compounds. This method has widely been used as the spin-trapping technique to identify the transient radicals in the fields of biochemistry, photochemistry, and polymer chemistry.[12] However, it should be noted that the reactions of alkyl radicals with nitroso compounds give aminoxyls (nitroxides) alone as the spin adducts. However, Konaka and Terabe found that, when 2,4,6-tri-*tert*-butylnitrosobenzene was used as a spin trapping agent, *N*-alkoxy-2,4,6-tri-*tert*-butylphenylaminyls were generated as the spin adducts, together with *N*-alkyl-2,4,6-tri-*tert*-butylphenylaminoxyls. They also found that the ratios of *N*-alkoxyaminyls to aminoxyls depended on the bulkiness of the attacking radicals.[13] *N*-Alkoxy-2,4,6-tri-*tert*-butylphenylaminyls react with oxygen, different from **1**−**3**, and nobody has succeeded in the isolation of them. Standing on this background, we investigated the reaction of 2,4,6-triphenylnitrosobenzene (**4a**), 2,4-diphenyl-6-*tert*-butylnitrosobenzene (**4b**), and 2,4-bis(4-chlorophenyl)-6-*tert*-butylnitrosobenzene (**4c**) with azo compounds **5a**−**c** in refluxing benzene. Although the reaction of **4a** with **5a**−**c** gave the corresponding aminoxyls alone as the spin adducts, the reaction of **4b** and **4c** with **5a**−**c** gave predominantly *N*-alkoxy-2,4-diaryl-6-*tert*-butylphenylaminyls, which were isolated as radical crystals. Herein, we wish to report a new methodology for the preparation of *N*-*tert*-alkoxyphenylaminyls and their isolation, ESR spectroscopic study, and magnetic properties.

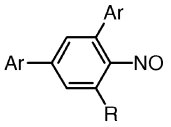

4

a: Ar = Ph, R = Ph
b: Ar = Ph, R = *t*-Bu
c: Ar = 4-ClC$_6$H$_4$, R = *t*-Bu

5

a: R = C(Me$_2$)COOCH$_3$
b: R = C(CN)(Me)CH$_2$CH(Me)CH$_3$
c: R = C(CN)(Me)CH$_2$C(OMe)(Me)CH$_3$

SCHEME 1

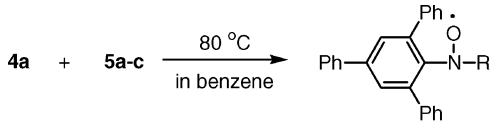

6

a: R = C(Me$_2$)COOCH$_3$
b: R = C(CN)(Me)CH$_2$CH(Me)CH$_3$
c: R = C(CN)(Me)CH$_2$C(OMe)(Me)CH$_3$

Results and Discussion

The azo compounds used in this study were **5a**−**c**, and their half-life times ($\tau_{1/2}$) in toluene are 80 min at 80 °C (**5a**), 10 min at 80 °C (**5b**), and about 3.5 min at 70 °C (**5c**),[14] respectively. The reactions of nitrosobenzenes with azo compounds were carried out in refluxing benzene under a nitrogen atmosphere.

Reactions of 2,4,6-Triphenylnitrosobenzene (4a) with Azo Compounds. The reactions of **4a** with **5a**−**c** were initially investigated (Scheme 1). When solutions of **4a** and 0.65−1.0 equiv of **5a** were heated in refluxing benzene for 0.5−4 h, the color of the solutions changed from light greenish blue to light yellow. The light blue color is due to the nitrosobenzene. After the mixtures were heated for a given time, the ESR signals from the mixtures were measured at room temperature. The observed spectrum was a 1:1:1 triplet and its a_N and g values were 1.274 mT and 2.0059, respectively. The a_N and g values are similar to those for aminoxyls **9a** and **9b** (a_N = 1.322−1.340 mT, g = 2.0062),[15−17] demonstrating that the observed radical is aminoxyl **6a**. In the same manner, the reactions of **4a** with **5b** and **5c** were carried out, and the ESR signals observed from the reaction mixtures showed that they were due to aminoxyls **6b** and **6c**. On the basis of the above ESR results, it is concluded that the reactions of **4a** with **5a**−**c** yield aminoxyls **6a**−**c** alone.

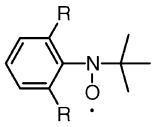

9

a: R = Me, **b**: R = OMe

Reactions of 2,4-Diaryl-6-*tert*-butylnitrosobenzene (4b) with 5a−c. When the mixtures of **4b** and **5a**−**c** were heated in refluxing benzene for 0.5−4.0 h (Scheme 2), the color of the mixtures changed from light greenish blue to deep red. This color change is different from those observed in the reactions of **4a** with **5a**−**c**. After cooling, the ESR spectra were measured. When a mixture of **4b** with 0.65 equiv of **5a** was heated for 1.0 h, two kinds of 1:1:1 triplet ESR signals were observed from the mixture, as shown in Figure 1. The a_N and g values for the triplet signal shown by *a* are 1.294 mT and 2.0061, respectively,

(3) Miura, Y. *Trends Org. Chem*. **1997**, *6*, 197−217; *Recent Res. Dev. Org. Chem*. **1998**, *2*, 251−268.
(4) Miura, Y.; Tomimura, T. *Chem. Commun.* **2001**, 627.
(5) Miura, Y.; Tomimura, T.; Matsuba, N.; Tanaka, R.; Nakatsuji, M.; Teki, Y. *J. Org. Chem*. **2001**, *66*, 7456.
(6) Miura, Y.; Matsuba, N.; Tanaka, R.; Teki, Y.; Takui, T. *J. Org. Chem*. **2002**, *67*, 8764.
(7) Miura, Y.; Nishi, T.; Teki, Y. *J. Org. Chem*. **2003**, *68*, 10158.
(8) Morita, Y.; Kawai, J.; Fukui, K.; Nakazawa, S.; Sato, K.; Shiomi, D.; Takui, T.; Nakasuji, K. *Org. Lett*. **2003**, *5*, 3289 and references therein.
(9) Zienkiewicz, J.; Kaszynski, P.; Young, V. G., Jr. *J. Org. Chem*. **2004**, *69*, 7525.
(10) *Magnetic Properties of Organic Materials*; Lahti, P. M., Ed.; Marcel Dekker: New York, Basel, 1999.
(11) A preliminary communication of the present work: Miura, Y.; Muranaka, Y. *Chem. Lett*. **2005**, *34*, 480.
(12) Janzen, E. G. *Acc. Chem. Res*. **1971**, *4*, 31,
(13) Terabe, S.; Konaka, R. *J. Chem. Soc., Perkin Tran. 2* **1973**, 369.
(14) Dixon, K. W. In *Polymer Handbook*, 4th ed.; Brandrup, J., Immergut, E. H., Grulke, E. A., Eds.; John Wiley & Sons: New York, 1999; pp II/1−II/76.
(15) Rozantsev, E. G. *Free Nitroxyl Radicals*; Plenum Press: New York and London, 1970. Forrester, A. R.; Hay, J. M.; Thomson, H. R. In *Organic Chemistry of Stable Free Radicals*; Academic Press: London and New York, 1968; Chapter 5. Volodarsky, L. B.; Reznikov, V. A.; Ovcharenko, V. I. *Synthetic Chemistry of Stable Nitroxides*; CRC Press: Boca Raton, 1994.
(16) Calder, A.; Forrester, A. R. *Chem. Commun*. **1967**, 682.
(17) Hoffmann, A. K.; Feldman, A. M.; Gelblum, E. *J. Am. Chem. Soc*. **1964**, *86*, 646.

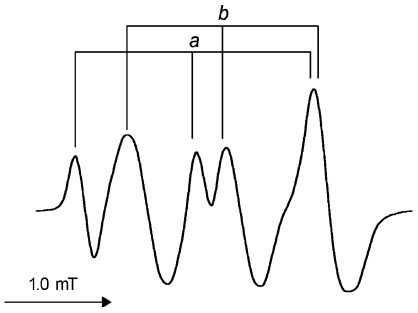

FIGURE 1. ESR spectrum recorded at room temperature after a mixture of **4b** and 0.65 equiv of **5a** in benzene was heated at 80 °C for 1 h. The observed **7a** and **8a** are shown by *b* and *a*, respectively.

SCHEME 2

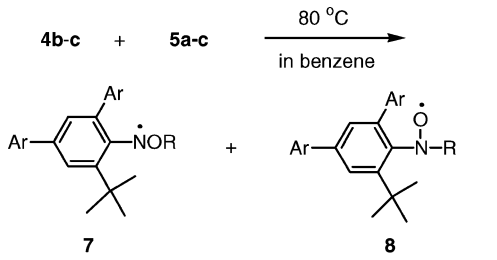

7a, **8a**: Ar = Ph, R = $C(Me_2)COOCH_3$
7b, **8b**: Ar = Ph, R = $C(CN)(Me)CH_2CH(Me)CH_3$
7c, **8c**: Ar = Ph, R = $C(CN)(Me)CH_2C(OMe)(Me)CH_3$
7d, **8d**: Ar = 4-ClC_6H_4, R = $C(CN)(Me)CH_2CH(Me)CH_3$

which indicate that it is aminoxyl **8a**. On the other hand, the a_N and g values for the triplet signal shown by *b* are 0.993 mT and 2.0039, respectively, which are very similar to those for **1**−**3** (a_N = 0.984−1.05 mT, g = 2.0041−2.0043). On the basis of the analogous ESR parameters, it is concluded that the later radical is the desired *N*-alkoxyphenylaminyl **7a**. The relative intensity of **7a** to **8a** determined by the double integration of the ESR signals is 3.7, which shows that **7a** is predominantly formed in the reaction of **4b** with **5a**. When a mixture of **4b** and 0.65 equiv of **5a** was heated for a longer time (2.0 and 4.0 h), the relative intensities of **7a** to **8a** increased to 5.4 and 9.5, respectively.

The above results prompted us to isolate **7a**. Because **7a** was inert to oxygen, similar to **1**−**3** and their analogues,[1,4−7] isolation of **7a** was quite easy; the red-colored reaction mixture was concentrated under reduced pressure, and the red zone was separated by column chromatography. Recrystallization from MeOH gave red needles. The results are summarized in Table 1. Table 1 shows that when the ratio for **5a**/**4b** is 0.65, the yields of **7a** are in the range from 20 to 37% (runs 1−3), and when the ratio is 1.0, the reaction mixtures give **7a** in 38−45% yield (runs 4 and 5). On the other hand, when the ratio is increased to 2.0, the yield decreases to 13% (run 6). Therefore, the use of a large excess of the azo compounds leads to a drastic reduction in the yield of **7a**.

The reactions of **4b** with **5b** were carried out in the same manner as above. Because the half-life time of **5b** is only 10 min (at 80 °C), the reaction time was shortened to 2 h or less. Upon heating, the reaction mixtures showed a strong ESR signal due to **7b**, while the signal due to **8b** was very weak or not observed. When the ratio for **5b**/**4b** is 0.65, the yields of **7b** are 27−44% (runs 7 and 8), and when the ratio for **5b**/**4b** is 1.0, the yields are increased to 46−49% (runs 9 and 10). However, when the ratio for **5b**/**4b** is 2.0, the yield of **7b** decreases to 18% (run 11), again indicating that the use of a large excess of azo compound drastically reduces the yield of **7b**.

TABLE 1. Results of the Reactions of 4b, 4c, 13a, and 13b with 5a−c[a]

run	azo compound[b] (mmol)	nitroso compound[c]	molar ratio of **5** to **4**	time (h)	isolated radical	yield[d] (%)
1	**5a** (0.515)	**4b**	0.65	1.0	**7a**	20
2	**5a** (0.515)	**4b**	0.65	2.0	**7a**	32
3	**5a** (0.515)	**4b**	0.65	4.0	**7a**	37
4	**5a** (0.793)	**4b**	1.0	4.0	**7a**	38
5	**5a** (0.793)	**4b**	1.0	6.0	**7a**	45
6	**5a** (1.59)	**4b**	2.0	4.0	**7a**	13
7	**5b** (0.515)	**4b**	0.65	1.0	**7b**	27
8	**5b** (0.515)	**4b**	0.65	2.0	**7b**	44
9	**5b** (0.793)	**4b**	1.0	0.5	**7b**	49
10	**5b** (0.793)	**4b**	1.0	1.0	**7b**	46
11	**5b** (1.59)	**4b**	2.0	1.0	**7b**	18
12	**5c** (0.515)	**4b**	0.65	0.5	**7c**	33
13	**5c** (0.793)	**4b**	1.0	0.5	**7c**	49
14	**5b** (0.793)	**4c**	0.65	1.0	**7d**	33
15	**5b** (0.793)	**4c**	1.0	1.0	**7d**	52
16	**5b** (0.793)	**4c**	1.0	2.0	**7d**	50
17	**5a** (0.793)	**13a**	1.0	4.0	**11**	36
18	**5a** (0.793)	**13b**	1.0	4.0	**12a**	33
19	**5b** (0.793)	**13b**	1.0	1.0	**12b**	49

[a] Benzene, 30 mL; temperature, 80 °C. [b] The $\tau_{1/2}$ of **5a** and **5b** in toluene at 80 °C are 80 and 10 min, respectively, and that of **5c** in toluene at 70 °C is about 3.5 min. [c] 0.793 mmol. [d] Isolated yields based on the nitrosobenzene.

Because the half-life time of **5c** is very short (>10 min at 80 °C), the mixtures of **4b** and **5c** were heated for only 0.5 h. The radicals detected from the reaction mixtures were **7c** alone. Table 1 shows that the reaction of **4b** with 0.65 equiv of **5c** gives **7c** in 33% yield (run 12), and the reaction of **4b** with 1.0 equiv of **5c** gives **7c** in 49% yield (run 13). Consequently, the yields of radicals are not different from those in the reactions of **4b** with **5a** or **5b**. The only difference is the shorter reaction time.

Influence of the Reaction Time on the Yields of 7a. To elucidate the influence of the reaction time on the yields of **7a** in more detail, the mixtures of **4b** and **5a** in *tert*-butylbenzene were heated to 80 °C in a degassed ESR tube set in an ESR cavity, and the concentrations of **7a** were plotted against time. The concentrations of **7a** were determined by the double integration of the ESR signals using tetramethylpiperidynyl-*N*-oxyl (TEMPO) as the reference. The results are shown in Figure 2. When **4b** was allowed to react with 1.0 equiv of **5a** (Figure 2a), the concentrations of **7a** increased with time and reached an almost constant concentration of 12.9 mmol L^{-1} at 7 h. The ESR yield of **7a** calculated from the radical concentration is 48%, which agrees with the isolated yield of 45% for the corresponding reaction (run 5) shown in Table 1. On the other hand, the yield of aminoxyl **8a** always remains below 4.3%, which suggests that the formed **8a** further reacts during the reaction. A plausible secondary reaction of **8a** may be the reversible reaction to nitrosobenzene **4b** and 2-(methoxycarbonyl)-2-propyl radical or the coupling reaction between of **8a** and 2-(methoxycarbonyl)-2-propyl radical. Unfortunately, TLC analysis of the reaction mixture gave no information about this point. When **4b** was allowed to react with 2.0 equiv of **5a** (Figure 2b), the concentration of **7a** increased with time and showed a maximum at 3 h. However, after that, it drastically decreased to 0.69 mol L^{-1}. The maximum ESR yield is 25%, and the yield at 4 h is only 14%. This yield agrees with the

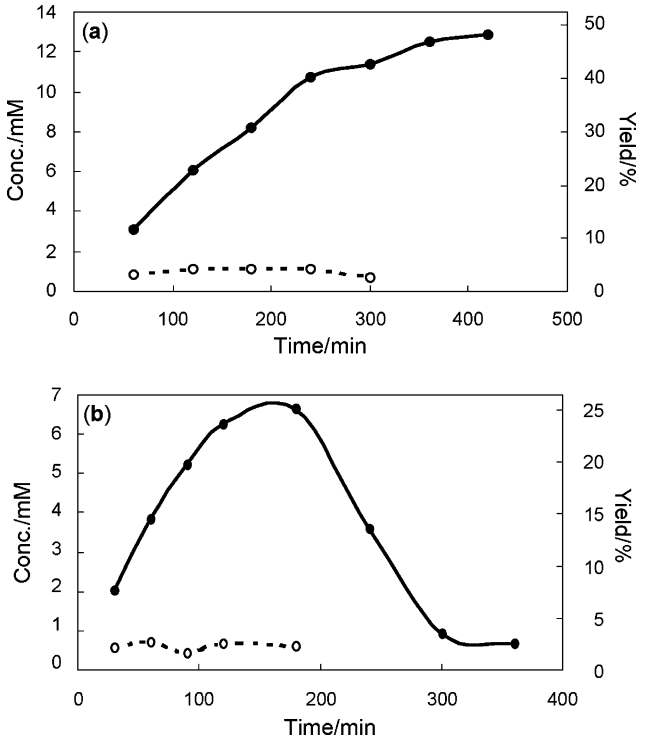

FIGURE 2. Plots of the ESR yields of **7a** and **8a** in the reaction of **4b** with **5a** at 80 °C against time. The yields of **7a** and **8a** are shown in solid and broken lines, respectively. (a) The **5a**/**4b** ratio is 1.0. (b) The **5a**/**4b** ratio is 2.0.

isolated yield of 13% for the corresponding reaction (run 6) shown in Table 1. Consequently, Figure 2b clearly shows that the use of a large excess of azo compounds leads to a drastic decrease in the yield of **7a**, in agreement with the results of runs 6 and 11 in Table 1. A possible reaction to reduce the yields of **7a** is the secondary reactions of **7** with *tert*-alkyl radicals as mentioned above. After a mixture of **4b** and 2.0 equiv of **5a** was heated for 6.0 h, the resultant mixture was analyzed with TLC. The TLC analysis showed the formation of many products. Although effort was made to identify possible products including **10** from the secondary reaction of **7a** with 2-methoxycarbonyl-2-propyl radical, no products were identified.

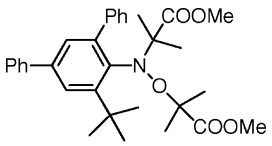

10

Generation and Isolation of Functional-Group-Carrying *N*-*tert*-Alkoxy-2,4-diaryl-6-*tert*-butylphenylaminyls. Because the present methodology does not use agents to react with functional groups, functional-group-carrying *N*-*tert*-alkoxy-2,4-diaryl-6-*tert*-butylphenylaminyls can be prepared by using the present method. We selected acetyl and cyano groups as functional groups, and acetyl-group-carrying *N*-*tert*-alkoxyarylaminyl **11** and cyano-group-carrying *N*-*tert*-alkoxyarylaminyls **12** were prepared using this method. The corresponding nitrosobenzenes **13a** and **13b** were prepared according to Scheme 3. When a mixture of **13a** and 1.0 equiv of **5a** was heated in refluxing benzene for 4 h, **11** was obtained in 36% yield. In the same manner, when a mixture of **13b** and 1.0 equiv of **5a**

SCHEME 3

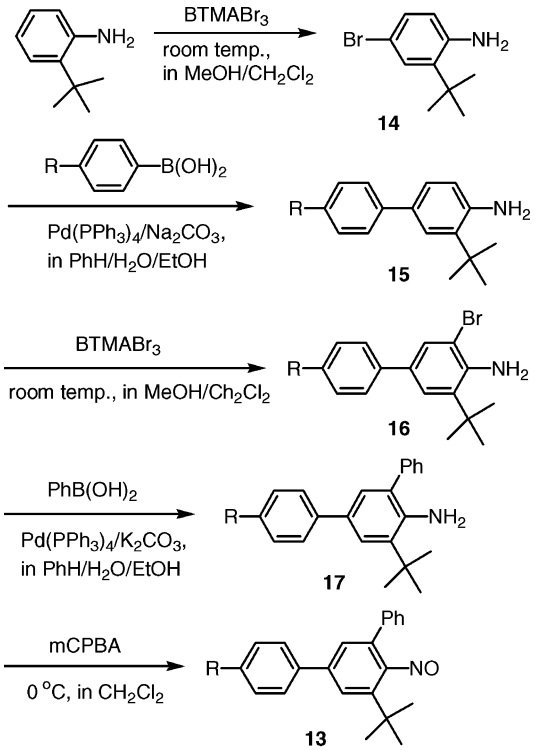

13a, **15a**-**17a**: R = CH_3CO
13b, **15b**-**17b**: R = CN

was heated for 4 h, **12a** was obtained in 33% yield, and when a mixture of **13b** and 1.0 equiv of **5b** was heated for 1 h, the reaction mixture gave **12b** in 49% yield. As found in Table 1, the yields of **11** and **12** are almost similar to those in the reactions of **4b** with **5a**−**c**, demonstrating that the present method can be applicable to the syntheses of functional-group-carrying radicals.

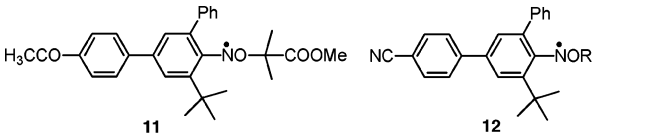

a: R = $C(Me_2)COOCH_3$
b: R = $C(CN)(Me)CH_2CH(Me)CH_3$

X-ray Crystallographic Analyses. Fortunately, because two radicals, **7c** and **7d**, gave good single crystals suitable for X-ray crystallographic analysis, the analyses were successfully performed for the two radicals. The molecular structures of **7c** and **7d** are illustrated in Figures 3 and 4. In the case of **7c**, the torsion angle for O1−N1−C1−C2 is −18.5(6)° (for O1−N1−C1−C6, 160.6(3)°), indicating that ring A defined by C1−C6 is fairly twisted from the NO radical center π system. This is in contrast to the X-ray results of **1** (Ar = Ph). The corresponding torsion angle of **1** is only −175.4(2)°, showing that N1, O1, and ring A are almost in the same plane. This difference may be ascribed to the difference in the bulkiness of the *tert*-alkoxy groups of **7c** and **1**. The dihedral angle between ring A and ring B defined by C7−C12 is 69.7°, suggesting that there is a large congestion around the NO radical center. On the other hand, the dihedral

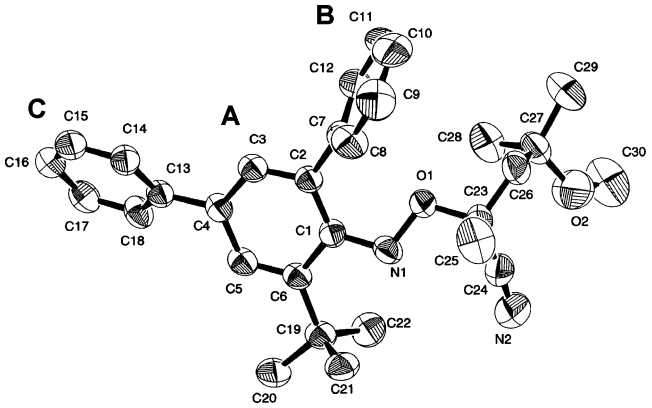

FIGURE 3. ORTEP drawing of **7c** at 50% probability. The selected bond lengths (Å), bond angles (°), and torsion angles (°) are as follows: N(1)−O(1), 1.382(4); O(1)−N(1)−C(1), 110.8(3); N(1)−O(1)−C(23), 111.0(3); O(1)−N(1)−C(1)−C(2), −18.5(6); O(1)−N(1)−C(1)−C(6), 160.6(3).

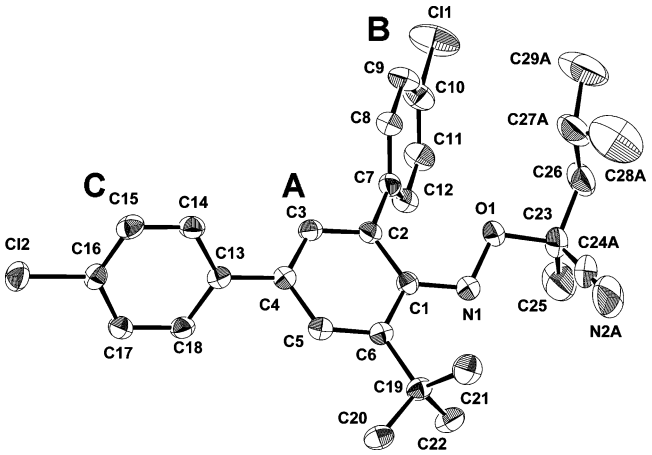

FIGURE 4. ORTEP drawing of **7d** at 50% probability. The selected bond lengths (Å), bond angles (°), and torsion angles (°) are as follows: N(1)−O(1), 1.386(3); O(1)−N(1)−C(1), 112.22 (19); N(1)−O(1)−C(23), 109.98 (19); O(1)−N(1)−C(1)−C(2), 13.9(3); O(1)−N(1)−C(1)−C(6), −164.20 (18).

angle between ring A and ring C defined by C13−C18 is 19.5°, suggesting that the unpaired electron spin can be delocalized onto the ring C to some extent. In the case of **7d**, the torsion angle between for O1−N1−C1−C2 is 13.9(3)° (for O1−N1−C1−C6, −164.20(18)°), which is smaller than that in **7c**, but indicates that ring A defined C1−C6 is fairly twisted from the NO radical center π system. On the other hand, the dihedral angles between ring A and ring B defined by C7−C12 and that between ring A and ring C defined by C13−C18 are 62.7 and 49.5°, respectively, suggesting that the delocalization of the unpaired electron spin onto rings B and C is a very small.

ESR Spectroscopy. ESR spectra of **7**, **11**, and **12** were measured at room temperature using benzene as the solvent. All the radicals measured (other than the deuterated radical) showed a broad 1:1:1 triplet, as illustrated in Figure 5. No resolution or quite poor resolution due to aromatic protons can be ascribed to the presence of numerous protons with unresolved small hyperfine coupling (hfc) constants. To obtain well-resolved

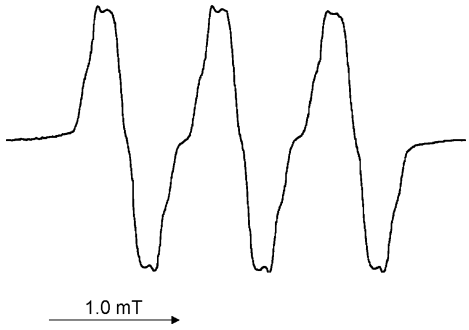

FIGURE 5. ESR spectrum of **7a** in benzene at room temperature.

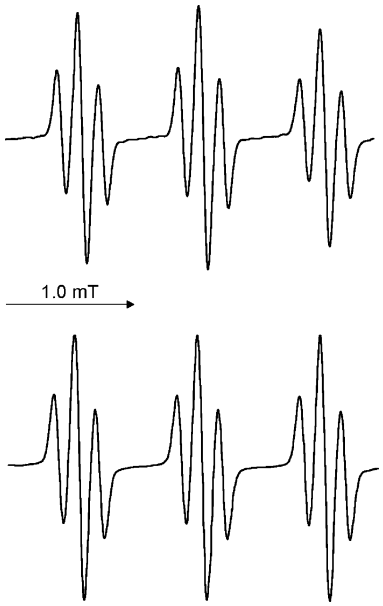

FIGURE 6. ESR spectrum of **7a-*d*$_{10}$** in benzene at room temperature. The a_N and a_H are determined by computer simulation.

ESR spectra, the 2- and 4-phenyl groups of **7a** were deuterated. The deuterated radical, **7a-*d*$_{10}$**, was prepared according to the

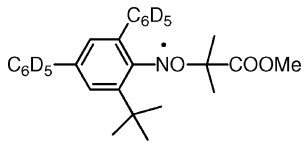

7a-*d*$_{10}$

same procedure as that for the nondeuterated radical. As found in Figure 6, the ESR spectrum is split into 1:2:1 triplets of a 1:1:1 triplet, from which a_N and a_H were determined to be 0.993 and 0.165 mT, respectively, by computer simulation. The hfc constants and g values for **7**, **11**, and **12** are summarized in Table 2, together with UV−vis spectral data. The a_N values are in the range of 0.965−1.01 mT, which are close to those for **1**−**3** (0.984−1.05 mT). The somewhat smaller a_Ns observed for **11** and **12** can be accounted for in terms of an increase in the relative importance of canonical form B as a result of the presence of an electron-withdrawing acetyl or cyano group (Scheme 4). The proton hyperfine splittings observed for **7a-*d*$_{10}$** are assigned to the aniline meta protons (2H).

TABLE 2. ESR and UV−Vis Data for 7, 11, and 12[a]

radical	hfc constant, mT	*g*	λ_{max}, nm (ϵ, L mol^{-1} cm^{-1})
7a	0.993[b]	2.0039	334 (30 800), 541 (1660)
7a-*d*$_{10}$[c]	0.993,[b] 0.165 (2H)[d]	2.0039	334 (29 400), 540.5 (1620)
7b	0.988[b]	2.0038	334 (27 300), 540 (1570)
7c	1.01[b]	2.0041	342 (25 800), 546 (1470)
7d	0.998[b]	2.0038	334 (26 200), 539 (1490)
11	0.985[b]	2.0041	359.5 (23 300), 534 (750)
12a	0.965[b]	2.0040	349 (32 600), 539 (900)
12b	0.973[b]	2.0039	352 (28 200), 544 (920)

[a] Solvent, benzene; room temperature (~25 °C). [b] The hfc constant for the NO nitrogen. [c] The hfc constants are determined by computer simulation. [d] The hfc constant for the aniline meta protons.

SCHEME 4

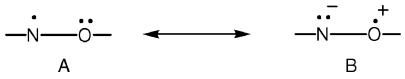

Spin Density Calculations. To discuss the spin density distribution in detail, the DFT calculations for **7d** were performed by the UB3LYP/6-31G(d) method using the geometry determined by X-ray crystallography.[18] The total atomic spin densities are illustrated in Figure 7, and some calculated hfc

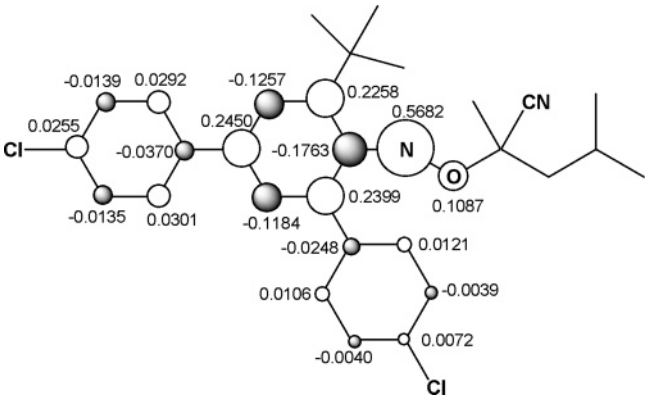

FIGURE 7. Total atomic spin densities of **7d** calculated by the UB3LYP/6-31G(d) method, using the geometry determined by X-ray crystallography.

constants are compared with the observed ones in Table 3. Table 3 shows that the calculated hfc constants are in good agreement with the observed ones. Relatively large spin densities are found on NO and the aniline benzene ring (ring A). While small spin densities are found on the 4-phenyl group (ring C), those on the 2-phenyl group (ring B) are negligibly small. This is due to a large twisting of ring B from the aniline benzene ring.

Magnetic Susceptibility Measurements. The magnetic susceptibility measurements were carried out using the poly-

(18) All DFT calculations were carried out using the following: Frisch, M. J.; Trucks, G. W.; Schlegel, H. B.; Scuseria, G. E.; Robb, M. A.; Cheeseman, J. R.; Zakrzewski, V. G.; Montgomery, J. A., Jr.; Stratmann, R. E.; Burant, J. C.; Dapprich, S.; Millam, J. M.; Daniels, A. D.; Kudin, K. N.; Strain, M. C.; Farkas, O.; Tomasi, J.; Barone, V.; Cossi, M.; Cammi, R.; Mennucci, B.; Pomelli, C.; Adamo, C.; Clifford, S.; Ochterski, J.; Petersson, G. A.; Ayala, P. Y.; Cui, Q.; Morokuma, K.; Malick, D. K.; Rabuck, A. D.; Raghavachari, K.; Foresman, J. B.; Cioslowski, J.; Ortiz, J. V.; Stefanov, B. B.; Liu, G.; Liashenko, A.; Piskorz, P.; Komaromi, I.; Gomperts, R.; Martin, R. L.; Fox, D. J.; Keith, T.; Al-Laham, M. A.; Peng, C. Y.; Nanayakkara, A.; Gonzalez, C.; Challacombe, M.; Gill, P. M. W.; Johnson, B. G.; Chen, W.; Wong, M. W.; Andres, J. L.; Head-Gordon, M.; Replogle, E. S.; Pople, J. A. *Gaussian 98*, revision A.9; Gaussian, Inc.: Pittsburgh, PA, 1998.

TABLE 3. Calculated Hyperfine Coupling Constants for 7d

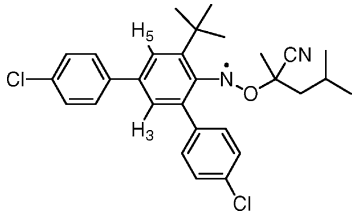

position	calcd hfc const[a,b]	obsd hfc const[a,b,c]
N[d]	1.081	0.998
O	−0.290	
H_3	0.223	0.165[e]
H_5	0.234	0.165[e]

[a] The hfc constants are given in mT. [b] The MO calculations are performed by the UB3LYP/6-31G(d) method. [c] Shown in the absolute values. [d] The NO nitrogen. [e] The proton hfc constants for **7d-*d*$_{10}$** are shown.

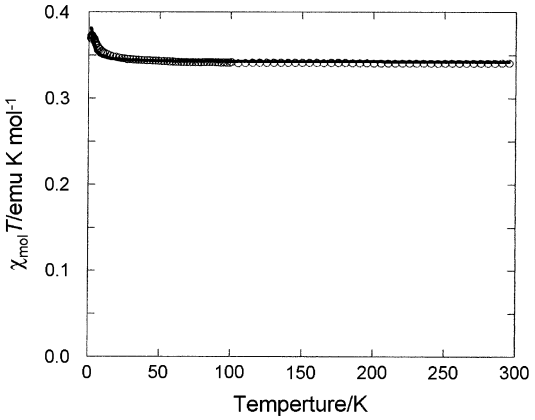

FIGURE 8. Plots of χT vs T for **7d**. The theoretical curve is drawn using the values calculated by the Curie−Weiss law.

crystalline samples of **7c** and **7d** in the temperature range 1.8−300 K with SQUID. The diamagnetic components were subtracted by the estimation based on Pascal's sum rule. The χ_{mol} (molar magnetic susceptibility) versus the $\chi_{mol}T$ plots for **7d** are depicted in Figure 8. The $\chi_{mol}T$ value at 300 K is 0.345 emu K mol^{-1}, from which the spin concentration is calculated to be 92% based on the theoretical value of 0.375 emu K mol^{-1} for the paramagnetic $S = 1/2$ spin system. The $\chi_{mol}T$ value is constant in the temperature range 300−12 K, and below 12 K, it increases slightly. This indicates that a weak ferromagnetic interaction operates between the neighboring radical molecules. The $\chi_{mol}T$ versus T plots were analyzed with the Curie−Weiss law (eq 1), and the Weiss temperature (θ) was determined to be +0.2 K.

$$\chi = \frac{C}{T - \theta} \tag{1}$$

The crystal structure of **7d** shows that the radical molecules are stacked along the *b* axis. Because the magnetic interaction is very weak, there may be some possible explanations for the weak ferromagnetic interaction. However, we found a plausible mechanism by the careful examination of the crystal structure of **7d**, as described below. The radicals interact through C16- - - C17′ and C17- - -C16′, with an intermolecular distance of 3.573 Å between the neighboring radicals, as shown in Figure 9. The

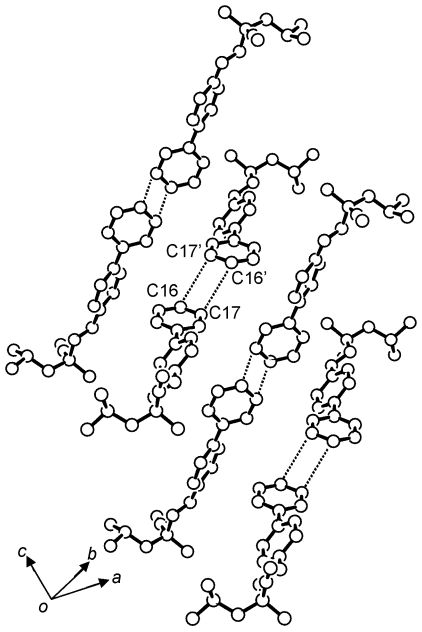

FIGURE 9. Stacking mode of **7d**. The dotted lines show the ferromagnetic interactions between two radical molecules. The distance between C16- - -C17′ (and C17- - -C16′) is 3.573 Å.

spin densities on C16 and C17 predicted by the DFT calculations are +0.0255 and −0.0139, respectively. According to the McConnell rule,[19] the magnetic interaction between the two radical molecules is ferromagnetic, which is in agreement the observed result. However, because the spin densities on C16 and C17 are very low, the ferromagnetic interaction is very weak.

On the other hand, the $\chi_{mol}T$ versus T plots of **7c** showed a weak antiferromagnetic behavior. The $\chi_{mol}T$ value was constant above ∼80 K, and below ∼80 K, it gradually decreased. Analysis of the $\chi_{mol}T$ versus T plots with the Curie−Weiss law showed −3.8 K as θ, indicating that the antiferromagnetic interaction was weak. To clarify the mechanism for the antiferromagnetic interaction, the crystal structure of **7c** was investigated in detail. Because many weak antiferromagnetic and weak ferromagnetic interactions were found between the neighboring radicals, it was difficult to determine the mechanism for the observed weak antiferromagnetic interaction between the neighboring radicals.

Conclusions

The reactions of 2,4,6-triphenyl- and 2,6-diaryl-6-*tert*-butylnitrosobenzenes with three kinds of azo compounds **5a**−**c** were carried out with a purpose to establish a new methodology for the synthesis of isolable stable *N*-alkoxyphenylaminyls. Although the reactions of 2,4,6-triphenylnitrosobenzene with **5a**−**c** in refluxing benzene gave aminoxyls alone, the reactions of 2,4-diaryl-6-*tert*-butylnitrosobenzenes with **5a**−**c** gave the desired *N*-alkoxyphenylaminyls **7**, which were isolated as the radical crystals in 18−52% yields. When the same procedure was used, functional-group-carrying *N*-alkoxyphenylaminyls were prepared and isolated as radical crystals. In conclusion, this method will serve as a useful procedure for the synthesis of stable *N*-alkoxyphenylaminyls.

(19) McConnell, H. M. *J. Chem. Phys.* **1963**, *39*, 1910.

Experimental Section

2,2′-Azobis[2-(methoxycarbonyl)propane] (**5a**), 2,2′-azobis(2-cyano-4-methylpentane) (**5b**), and 2,2′-azobis(2-cyano-4-methyl-4-methoxypentane) (**5c**) were commercially available. 2,4,6-Triphenylnitrosobenzene (**4a**), 2,4-diphenyl-6-*tert*-butylnitrosobenzene (**4b**), and 2,4-di(phenyl-d_5)-6-*tert*-butylnitrosobenzene (**4b-d_{10}**) were prepared according to the reported methods.[5] Silica gel column chromatography was performed on silica gel 60 N (purchased from a commercial supplier), while alumina column chromatography was carried out on aluminum oxide 90 (purchased from a commercial supplier).

ESR Study. ESR spectra were measured with a Bruker ESP 300. Hyperfine splitting constants and g values were determined by the comparison with Fremy's salt in dilute K_2CO_3 aqueous solution (a_N = 1.309 mT, g = 2.0055).

In the kinetic ESR study, the relative concentrations of *N*-alkoxyaminyls and aminoxyls during the reactions were determined by the double integration of one peak in the lowest magnetic field of the corresponding 1:1:1 triplets ESR signals. After the measurements were finished, the ESR cells were immediately cooled to room temperature, and the individual concentrations of *N*-alkoxyaminyls and aminoxyls were determined using the calibration curves drawn by using the known concentration *tert*-butylbenzene solutions of TEMPO.

Magnetic Susceptibility Measurements. Magnetic susceptibility measurements were carried out using polycrystalline samples in the temperature range 1.8−300 K. The diamagnetic components were subtracted by the estimation based on Pascal's sum rule.

2-*tert*-Butyl-4-(4-acetylphenyl)aniline (15a). A mixture of 3.96 g (17.4 mmol) of 2-*tert*-butyl-4-bromoaniline, 4.80 g (29.3 mmol) of 4-acetylphenylboronic acid, 1.20 g (1.04 mmol) of $Pd(PPh_3)_4$, and 7.37 g of Na_2CO_3 in 112 mL of benzene, 32 mL of EtOH, and 44 mL of water was refluxed for 24 h with stirring under N_2. After cooling to room temperature, the mixture was extracted with benzene, and the combined benzene extracts were washed with brine, dried over anhydrous $MgSO_4$, and evaporated. The residue was then chromatographed on silica gel with 2:3 EtOAc−hexane to give **15a** in 65% yield (3.01 g, 11.3 mmol). Recrystallization from EtOH gave light yellow needles with mp 151−153 °C. ^{1}H NMR ($CDCl_3$) δ 1.48 (s, 9H), 2.62 (s, 3H), 4.00 (br s, 2H), 6.77 (d, J = 8.0 Hz, 1H), 7.35 (dd, J = 8.0 and 2.4 Hz, 1H), 7.54 (d, J = 2.4 Hz, 1H), 7.63 (d, J = 8.2 Hz, 2H), 7.99 (d, J = 8.2 Hz, 2H). Anal. Calcd for $C_{18}H_{21}NO$: C, 80.86; H, 7.92; N, 5.24. Found: C, 80.95; H, 7.99; N, 5.24.

2-Bromo-4-(4-acetylphenyl)-6-*tert*-butylaniline (16a). A mixture of 3.00 g (11.2 mmol) of **15a**, 5.24 g (13.4 mmol) of benzyltrimethylammonium tribromide ($BTMABr_3$), and 1.46 g of $CaCO_3$ in 100 mL of CH_2Cl_2 and 35 mL of MeOH was stirred for 4 h at room temperature. After filtration, the CH_2Cl_2 layer was washed with aqueous $NaHSO_3$ and then brine, dried over anhydrous $MgSO_4$, and evaporated. The residue was then chromatographed on silica gel with benzene. Recrystallization from EtOH gave **16a** as colorless needles in 96% yield (3.72 g, 10.7 mmol). Mp 116−117 °C; ^{1}H NMR ($CDCl_3$) δ 1.48 (s, 9H), 2.63 (s, 3H), 4.57 (br s, 2H), 7.47 (d, J = 2.0 Hz, 1H), 7.60 (d, J = 8.4 Hz, 2H), 7.66 (d, J = 2.0 Hz, 1H), 7.99 (d, J = 8.4 Hz, 2H). Anal. Calcd for $C_{18}H_{20}$-BrNO: C, 62.44; H, 5.82; N, 4.05. Found: C, 62.43; H, 5.81; N, 3.87.

2-Phenyl-4-(4-acetylphenyl)-6-*tert*-butylaniline (17a). A mixture of 3.41 g (9.84 mmol) of **16a**, 1.56 g (12.8 mmol) of phenylboronic acid, 0.683 g (0.591 mmol) of $Pd(PPh_3)_4$, and 5.44 g of K_2CO_3 in 100 mL of benzene, 45 mL of water, and 20 mL of EtOH was refluxed for 24 h with stirring under N_2. After cooling, water was added, and the mixture was extracted with benzene. After the combined benzene extracts were washed with brine and dried over anhydrous $MgSO_4$, the solvent was evaporated under reduced pressure and the residue was chromatographed on silica gel with 1:8 EtOAc−hexane. Recrystallization from EtOH gave **17a** as

colorless needles in 83% yield (2.81 g, 8.18 mmol). Mp 168−170 °C; ^{1}H NMR ($CDCl_3$) δ 1.53 (s, 9H), 2.62 (s, 3H), 4.13 (br s, 2H), 7.32 (d, J = 2.4 Hz, 1H), 7.38−7.41 (m, 1H), 7.48 (d, J = 4.4 Hz, 4H), 7.58 (d, J = 2.4 Hz, 1H), 7.66 (d, J = 8.4 Hz, 2H), 7.98 (d, J = 8.4 Hz, 2H). Anal. Calcd for $C_{24}H_{25}NO$: C, 83.93; H, 7.34; N, 4.08. Found: C, 83.72; H, 7.22; N, 4.00.

2-Phenyl-4-(4-acetylphenyl)-6-*tert*-butylnitrosobenzene (13a). A solution of 1.96 g (5.71 mmol) of **17a** in 25 mL of CH_2Cl_2 was cooled to 0 °C with stirring, and a solution of 2.76 g (16.0 mmol) of *m*-chloroperbenzoic acid in 30 mL of CH_2Cl_2 was added dropwise for 15 min. After the completion of the addition, the mixture was raised to room temperature with stirring and 100 mL of water was added. The CH_2Cl_2 layer was washed with brine, dried over anhydrous $MgSO_4$, and evaporated under reduced pressure. The residue was then chromatographed on silica gel with 1:8 benzene−EtOAc to give **13a** as green microneedles containing small amounts of impurities. Accordingly, the compound was further purified with a recycling preparative HPLC instrument with $CHCl_3$ as the eluent. Yield 70% (1.42 g, 3.97 mmol); mp 106−108 °C; ^{1}H NMR ($CDCl_3$) δ 1.72 (s, 9H), 2.66 (s, 3H), 6.83−6.86 (m, 2H), 7.24 (d, J = 2.0 Hz, 1H), 7.32−7.34 (m, 3H), 7.74 (d, J = 8.4 Hz, 2H), 7.89 (d, J = 2.0 Hz, 1H), 8.06 (d, J = 8.4 Hz, 2H). Anal. Calcd for $C_{24}H_{23}NO_2$: C, 80.64; H, 6.49; N, 3.92. Found: C, 80.78; H, 6.34; N, 3.83.

***N*-[2-(Methoxycarbonyl)-2-propoxy]-2-phenyl-4-(4-acetylphenyl)-6-*tert*-butylphenylaminyl (11).** A solution of 200 mg (0.56 mmol) of **13a** and 129 mg (0.56 mmol) of **5a** in 30 mL of benzene was refluxed for 4 h under a N_2 atmosphere. The red mixture was evaporated under reduced pressure, and the residue was chromatographed on silica gel with 1:4 EtOAc−hexane to give **11** in 36% yield (131 mg, 0.286 mmol). Recrystallization from MeOH gave red needles with mp 125−127 °C. Anal. Calcd for $C_{29}H_{32}NO_4$: C, 75.96; H, 7.03; N, 3.05. Found: C, 75.84; H, 6.96; N, 2.79.

2-*tert*-Butyl-4-(4-cyanophenyl)aniline (15b). A mixture of 3.80 g (16.5 mmol) of 2-*tert*-butyl-4-bromoaniline, 4.41 g (30.0 mmol) of 4-cyanophenylboronic acid, 0.577 g (0.50 mmol) of $Pd(PPh_3)_4$, and 7.1 g of Na_2CO_3 in 112 mL of benzene, 32 mL of EtOH, and 44 mL of water was refluxed for 24 h with stirring under N_2. After cooling to room temperature, the mixture was extracted with benzene and the combined benzene extracts were washed with brine, dried over anhydrous $MgSO_4$, and evaporated. The residue was then chromatographed on silica gel with 1:6 EtOAc−hexane to give **15b** in 49% yield (2.01 g, 8.03 mmol). Recrystallization from EtOH gave colorless plates with mp 112−114 °C. ^{1}H NMR ($CDCl_3$) δ 1.47 (s, 9H), 4.02 (br s, 2H), 6.73 (d, J = 8.3 Hz, 1H), 7.30 (dd, J = 8.3 and 2.2 Hz, 1H), 7.48 (d, J = 2.2 Hz, 1H), 7.62 (d, J = 8.3 Hz, 2H), 7.66 (d, J = 8.3 Hz, 2H). Anal. Calcd for $C_{17}H_{18}N_2$: C, 81.56; H, 7.25, N, 11.19. Found: C, 81.47; H, 7.14; N, 11.28.

2-Bromo-4-(4-cyanophenyl)-6-*tert*-butylaniline (16b). A mixture of 0.944 g (3.77 mmol) of **15b**, 1.76 g (4.52 mmol) of $BTMABr_3$, and 0.49 g of $CaCO_3$ in 32 mL of CH_2Cl_2 and 10 mL of MeOH was stirred for 2 h at room temperature. After filtration, the CH_2Cl_2 layer was washed with aqueous $NaHSO_3$ and then brine, dried over anhydrous $MgSO_4$, and evaporated. The residue was then chromatographed on silica gel with 1:4 EtOAc−hexane and recrystallization from EtOH gave **16b** as colorless needles in 86% yield (1.07 g, 3.25 mmol). Mp 148−150 °C; ^{1}H NMR ($CDCl_3$) δ 1.48 (s, 9H), 4.60 (br s, 2H), 7.43 (d, J = 2.0 Hz, 1H), 7.60 (d, J = 8.2 Hz, 2H), 7.62 (d, J = 2.0 Hz, 1H), 7.68 (d, J = 8.2 Hz, 2H). Anal. Calcd for $C_{17}H_{17}BrN_2$: C, 62.02; H, 5.20; N, 8.51. Found: C, 61.98; H, 5.15; N, 8.44.

2-Phenyl-4-(4-cyanophenyl)-6-*tert*-butylaniline (17b). A mixture of 1.42 g (4.31 mmol) of **16b**, 0.684 g (5.61 mmol) of phenylboronic acid, 0.299 g (0.259 mmol) of $Pd(PPh_3)_4$, and 2.4 g of K_2CO_3 in 43 mL of benzene, 19 mL of water, and 9 mL of EtOH was refluxed for 24 h with stirring under N_2. After cooling, water was added and the mixture was extracted with benzene. After the combined benzene extracts were washed with brine and dried over anhydrous $MgSO_4$, the solvent was evaporated under reduced pressure and the residue was chromatographed on silica gel with 1:4 EtOAc−hexane. Recrystallization from hexanes−EtOAc gave **17b** as light yellow needles in 69% yield (0.972 g, 2.98 mmol). Mp 141−143 °C; ^{1}H NMR ($CDCl_3$) δ 1.52 (s, 9H), 4.16 (br s, 2H), 7.27 (d, J = 2.0 Hz, 1H), 7.36−7.50 (m, 5H), 7.53 (d, J = 2.0 Hz, 1H), 7.65 (s, 4H). Anal. Calcd for $C_{23}H_{22}N_2$: C, 84.63; H, 6.79; N, 8.58. Found: C, 84.59; H, 6.80; N, 8.58.

2-Phenyl-4-(4-cyanophenyl)-6-*tert*-butylnitrosobenzene (13b). A solution of 0.688 g (2.11 mmol) of **17b** in 10 mL of CH_2Cl_2 was cooled to 0 °C with stirring, and a solution of 1.02 g (5.90 mmol) of *m*-chloroperbenzoic acid in 10 mL of CH_2Cl_2 was added dropwise for 15 min. After the completion of the addition, the mixture was raised to room temperature with stirring and 50 mL of water was added. The CH_2Cl_2 layer was washed with brine, dried on anhydrous $MgSO_4$, and evaporated under reduced pressure. The residue was then chromatographed on silica gel with 1:8 benzene−EtOAc, and crystallization from EtOH gave **13b** as green needles in 92% yield (0.664 mg, 1.95 mmol). Mp 128−130 °C; ^{1}H NMR ($CDCl_3$) δ 1.70 (s, 9H), 6.81−6.84 (m, 2H), 7.21 (d, J = 2.0 Hz, 1H), 7.34−7.34 (m, 3H), 7.73 (d, J = 8.5 Hz, 2H), 7.76 (d, J = 8.8 Hz, 2H), 7.84 (d, J = 2.0 Hz, 1H). Anal. Calcd for $C_{23}H_{20}N_2O$: C, 81.15; H, 5.92; N, 8.23. Found: C, 80.79; H, 5.90; N, 8.21.

***N*-[2-(Methoxycarbonyl)-2-propoxy]-2-phenyl-4-(4-cyanophenyl)-6-*tert*-butylphenylaminyl (12a).** A solution of 250 mg (0.734 mmol) of **13b** and 169 mg (0.743 mmol) of **5a** in 30 mL of benzene was refluxed for 4 h under a N_2 atmosphere. The red mixture was evaporated under reduced pressure, and the residue was chromatographed on silica gel with 1:4 ethyl acetate−hexane to give **12a** in 33% yield (102 mg, 0.231 mmol). Recrystallization from MeOH gave red needles with mp 154−156 °C. Anal. Calcd for $C_{28}H_{29}N_2O_3$: C, 76.16; H, 6.62; N, 6.34. Found: C, 76.10; H, 6.62; N, 6.33.

***N*-(2-Cyano-4-methyl-2-pentoxy)-2-phenyl-4-(4-cyanophenyl)-6-*tert*-butylphenylaminyl (12b).** A solution of 270 mg (0.793 mmol) of **13b** and 128 mg (0.793 mmol) of **5b** in 30 mL of benzene was refluxed for 1 h under a N_2 atmosphere. The red mixture was evaporated under reduced pressure, and the residue was chromatographed on alumina with 1:16 ethyl acetate−hexane to give **12b** in 49% yield (175 mg, 0.388 mmol). Recrystallization from MeOH gave red needles with mp 131−133 °C. Anal. Calcd for $C_{30}H_{32}N_3O$: C, 79.97; H, 7.16; N, 9.34. Found: C, 79.97; H, 7.17; N, 9.30.

X-ray Crystallography. All measurements were made on a Rigaku/MSC Mercury CCD diffractometer with graphite monochromated MoKα (λ = 0.710 70 Å) radiation, and the X-ray crystallographic data were collected at −50 °C. The structure of **7c** was solved by direct methods (SRI92).[20] The methoxy group showed disorders over two sites with an occupancy of 0.5. The ORTEP drawing shown in Figure 3 is one of them. Refinement of the structure was carried out on F^2 by full-matrix, least-squares method. The non-hydrogen atoms were refined anisotropically, and the hydrogen atoms were placed in the fixed position and not refined. All calculations were performed using the teXsan crystallographic software package.[21] On the other hand, the structure of **7d** was solved by direct methods using the SHELX 97 software package.[22] In **7d**, the C30−C32 group and the cyano group exhibited disorder over two sites with an occupancy of 0.5. The ORTEP drawing shown in Figure 4 is one of them. Refinement of the structure was carried out on F^2 by full-matrix, least-squares method using the SHELX 97 software package.[23] The nonhydrogen

(20) Altomare, A.; Burla, M. C.; Camalli, M.; Cascarano, M.; Giacovazzo, C.; Guagliardi, A.; Polidori, G. *J. Appl. Crystallogr.* **1994**, *27*, 435.

(21) *TeXsan*; Crystal Structure Analysis Package; Molecular Structure Corporation: The Woodlands, TX, 1985 and 1999.

(22) Sheldrick, G. M. *SHELXS97*; Program for Crystal Structure Solution; University of Göttingen: Göttingen, Germany, 1997.

(23) Sheldrick, G. M. *SHELXL97*; Program for Crystal Structure Refinement; University of Göttingen, Göttingen, Germany, 1997.

atoms were refined anisotropically, and the hydrogen atoms were placed in ideal positions and refined as riding atoms. $R1 = \Sigma||F_o| - |F_c||/\Sigma|F_o|$, $wR2 = [(\Sigma w(F_o^2 - F_c^2)^2/\Sigma w(F_o^2)^2)]^{1/2}$.[24]

Crystal Data. 7c: $C_{30}H_{35}N_2O_2$; formula weight, 455.62; monoclinic, space group $P2_1/n$(#14); $a = 10.470(2)$, $b = 36.980(6)$, $c = 6.8100(8)$ Å; $\beta = 97.120(7)°$; $V = 2616.4(7)$ Å^3; $Z = 4$; $D_{calcd} = 1.157$ g cm^{-3}; $F(000) = 980.00$; $\mu = 0.72$ cm^{-1}; crystal size $= 0.06 \times 0.05 \times 0.35$ mm; $2\theta_{max} = 55.0°$; reflections collected, 20 344; unique, 5929 ($R_{int} = 0.071$); parameter, 317; $R1 = 0.0996$ (for $I > 2.30\sigma(I)$); $wR2 = 0.179$; GOF $= 1.68$.

(24) The crystal structure data for radicals **6c** and **6d** have been deposited at the Cambridge Database: CCDC numbers 261609 and 294749, respectively. Copies of the data can be obtained free of charge via www.ccdc.cam.ac.uk/retrieving.html.

7d: $C_{29}H_{31}Cl_2N_2O$; formula weight, 494.46; monoclinic, space group $C2/c$(#15); $a = 49.366(5)$, $b = 9.5302(9)$, $c = 11.4601(11)$ Å; $\beta = 98.786(5)°$; $V = 5412.0(9)$ Å^3; $Z = 8$; $D_{calc} = 1.214$ g cm^{-3}; $F(000) = 2088.00$; $\mu = 2.63$ cm^{-1}; crystal size $0.25 \times 0.48 \times 0.07$ mm; $2\theta_{max} = 55.0°$; reflections collected, 20 023; unique, 6086 ($R_{int} = 0.0456$); parameter, 332; $R1 = 0.0750$ (for $I > 2.0\sigma(I)$); $wR2 = 0.1646$ (all data); GOF $= 1.183$.

Supporting Information Available: The synthetic procedures of **4c** and **7a**−**d** and their analytical data. The CIF files containing X-ray structural data of **7c** and **7d**. This material is available free of charge via the Internet at http://pubs.acs.org.

JO0600959